High-Uniformity Full-Color Waveguides Fabricated by Nanoimprint Lithography for Near-Eye Display

Yu-Ting Hu, Ming-Jui Wang, Seok-Lyul Lee, and Yu-Chieh Lin
AUO Corporation,
Hsinchu Science Park, Hsinchu, Taiwan, 300094, R.O.C

Abstract
Surface relief gratings offer the advantages of well-defined structure and can be mass produced using Nanoimprint Lithography (NIL). In this article, we propose an optimal folding partition design and fabricate a waveguide using NIL. After prototyping, we achieved a full-color waveguide delivering up to 880 nits/lumen and high uniformity, demonstrating its potential for applications in AR glasses.

Author Keywords
Augmented Reality; Waveguide; Surface Relief Grating; Efficiency; Full-color; Brightness Uniformity; Nanoimprint

1. Introduction
In recent years, the development and application of augmented reality (AR) technology have garnered significant attention and importance. With the increasing market demand for AR products, a growing number of AR-related products and applications have emerged, among which optical waveguide technology serves as a crucial component for AR glasses. Compared to traditional geometrical waveguides, diffractive waveguides offer design advantages that are more compact [1-4].

The selection of diffractive elements can be achieved through various techniques, including but not limited to surface relief grating (SRG), holographic optical element (HOE), and polarized volume grating (PVG) [5,6]. Among these, surface relief grating (SRG) are favored for their excellent dimensional definition and clear grating structures, allowing for precise optimization of coupling efficiency distribution during complex pupil scenarios. Furthermore, by integrating nanoimprint lithography, SRG can achieve high transfer rates through the imprinting of molds and photoresist materials, which provides good reproducibility and mass production capabilities that are crucial for high-performance AR products [7].

As the requirements for module design become increasingly stringent, particularly concerning compactness and lightweight configurations, the thickness of the waveguide must correspondingly decrease. Therefore, effectively distributing energy in the grating design becomes a central challenge in ensuring uniform brightness performance [8,9]. In this paper, we explore a method termed 'partition design of the folding,' which aims to optimize the energy distribution during light transmission to enhance brightness uniformity.

Specifically, our research objective is to achieve a 30-degree field of view (FOV) and uniformities of 42.5%, 41.0%, and 20.1% in RGB full-color images, while achieving a maximum efficiency of 880 nits/lm. Ultimately, we fabricated molds and successfully imprinted grating nanostructures, with experimental results aligning with our design predictions, demonstrating the effectiveness and potential application of our method.

2. AR Waveguide Optical System
The energy distribution logic is primarily guided by the arrangement of the varying grating structures, which determine the propagation efficiency and distribution of light within the waveguide. This setup typically includes folding and out-coupling gratings, designed to perform Exit Pupil Expansion (EPE) by enabling multiple bounces of light through the two grating elements to replicate the size of the exit pupil. As illustrated in Figure 1, the expanded pupil configuration allows the pupil to undergo repeated bounces within the waveguide between the folding and out-coupling regions, ultimately achieving effective pupil expansion. With a 45-degree grating angle, light is expanded in the Y direction at the folding grating, while the out-coupling grating expands in the orthogonal X direction, as shown in Figure 1(a).

To minimize energy loss during the propagation process and ensure efficient performance, effective structural variations must be implemented between the folding and out-coupling gratings to achieve optimal energy efficiency distribution. Figure 2 illustrate the energy distribution of the grating configuration in Figure 1(a). Figure 2(a) shows the height distribution of the folding grating structure in both the Y and X directions, showcasing different height variations in the Y direction while maintaining a constant height in the X direction. In contrast, Figure 2(b) presents the height distribution schematic of the out-coupling grating, which exhibits height variations in the X direction, while the height remains unchanged in the Y direction.

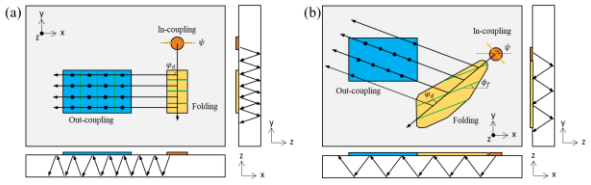

Figure 1. Encompasses the structural configuration of the In-coupling, folding, and out-coupling regions. It consists of two parts: (a) the grating angle at 45 degrees and (b) the grating angle at 60 degrees

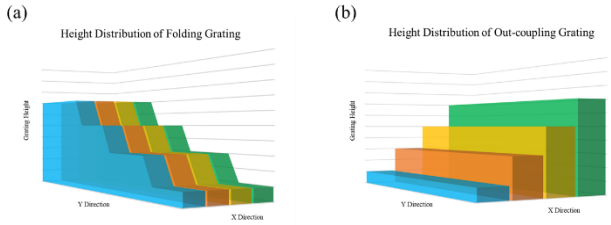

Figure 2. Height distribution of the grating structures in the X and Y directions for the waveguide configuration shown in Figure 1(a). (a) represents the folding grating, and (b) represents the out-coupling grating.

ISSN 0097-996X/25/5601-0402-$1.00 © 2025

On the other hand, we investigated the impact of efficiency discontinuity effects on the user's visual experience. This effect typically arises from variations in light extraction efficiency caused by different grating structures, particularly in the out-coupling grating region, which can lead to visual discomfort. As illustrated in Figure 3, the presence of the efficiency discontinuity effect is prominently displayed in the image. To address this issue, we introduced a folding partition design aimed at circumventing problems caused by the disparate grating structures in the exit pupil area, thereby enhancing overall viewing comfort.

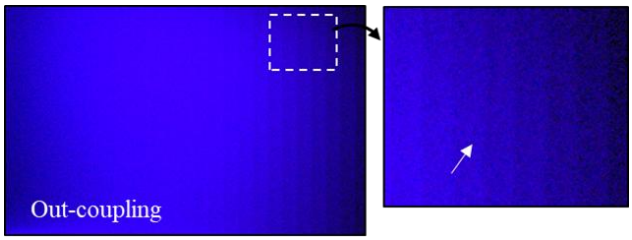

Figure 3. Out-coupling-coupling grating exhibiting the efficiency discontinuity effect

As shown in Figure 4, during the process of implementing the folding partition design, a light source with a wavelength of 525 nm and a field of view (FOV) of 30 degrees is used to incident light into a waveguide medium with a refractive index of 1.8. The In grating has an azimuthal angle of 130 degrees and a period of 480 nm. Since different FOVs correspond to different diffraction angles, the folding grating design is divided into various regions. Here, α and β represent the boundary angles of light diffraction, while $\alpha 1$ and $\beta 1$ represent the proportions of the diffraction angles in the XY direction. These proportions are derived from the relationship between the viewing angle θ, the azimuthal angle ψ of the In grating, the grating period d, and the wavelength λ.

Based on these parameters, we can derive the optimal partition direction of the folding grating, denoted as ϕf, using the following formula:

$$\boldsymbol{\phi_f = tan^{-1}(\frac{\beta_1}{\alpha_1})}$$

Here, the definitions of α_1 and β_1 are as follows:

$$\boldsymbol{\alpha_1 = (\frac{\lambda \sin\psi + \alpha d}{nd})} \text{ 、} \boldsymbol{\beta_1 = (\frac{\lambda \cos\psi + \beta d}{nd})}$$

Meanwhile, $\boldsymbol{\alpha}$ and $\boldsymbol{\beta}$ can be expressed as:

$$\boldsymbol{\alpha = \sin\frac{\theta}{2} \times \cos\psi \text{ 、 } \beta = \sin\frac{\theta}{2} \times \sin\psi}$$

As shown in Figure 5 (a-b), there is no partitioning in the out-coupling grating region, and the grating structures maintain consistency in both the Y and X directions. This design allows light to pass through this area without noticeable discontinuities, thereby reducing visual discomfort caused by changes in the grating structure (i.e., eliminating the efficiency discontinuity effect). As illustrated in Figure 6, the energy distribution on the out-coupling grating enables a smooth transition between various regions, maintaining consistency in efficiency.

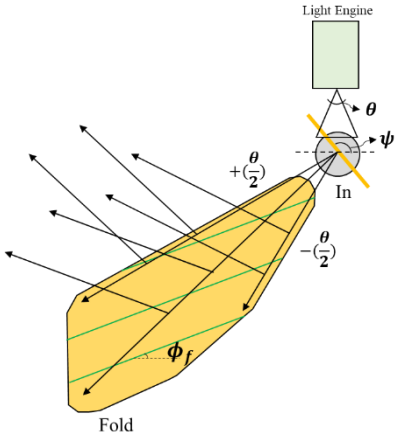

Figure 4. Schematic diagram of the parameters for the folding partition design.

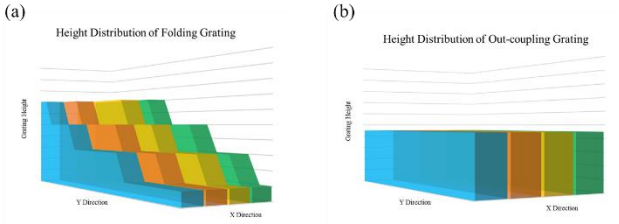

Figure 5. Height distribution of the grating structures in the X and Y directions for the waveguide configuration shown in Figure 1(b). (a) represents the folding grating, and (b) represents the out-coupling grating.

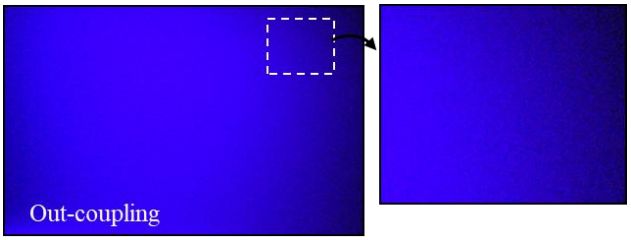

Figure 6. Out-coupling grating without the efficiency discontinuity effect.

In addition, this study not only avoids the efficiency discontinuity effect caused by the partitioning of the out-coupling grating but also enhances the uniformity of the two-dimensional image through the efficiency distribution of a single grating. Compared to unoptimized partitioning methods, as shown in Figure 7(a), the efficiency partitioning direction of the folding grating is aligned with the propagation direction of the R0 order light. Therefore, when light is coupled from the in-coupling grating into the folding grating structure and then generates the R-1 order light propagating to the out-coupling grating, the trajectory experiences only 2 to 5 efficiency modulations, as illustrated in Figure 8(a). This significantly reduces the spatial distribution of efficiency, leading to rapid energy loss during propagation and making it difficult to ensure satisfactory exit pupil efficiency performance in both directions.

As shown in Figure 7(b), the folding partition angle formula design in this study allows the partitioned regions to cover the light propagation paths and be adjusted according to specific optical requirements, ensuring that light maintains optimal

diffraction efficiency modulation when entering different regions. Consequently, even with only 4 zones of different efficiency configurations, each light beam with varying fields of view (FOV) in this system will, on average, undergo more than 5 to 8 adjustments of grating efficiency, as illustrated in Figure 8(b). This not only enhances the effective utilization of light at different angles and positions but also promotes overall brightness uniformity of the system. In this configuration, the grating designs for different regions are specifically optimized for their corresponding incident angles and light paths, achieving the best light redistribution effects.

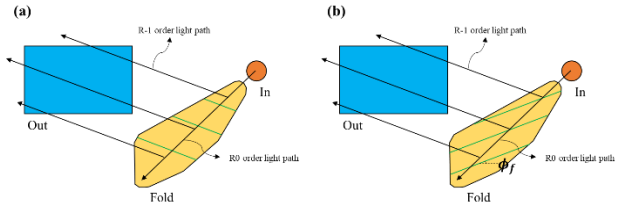

Figure 7. Folding grating partitioning methods. (a) represents the partitioning based on the propagation path of the R0 grating, while (b) illustrates the partitioning method designed according to the partition angles.

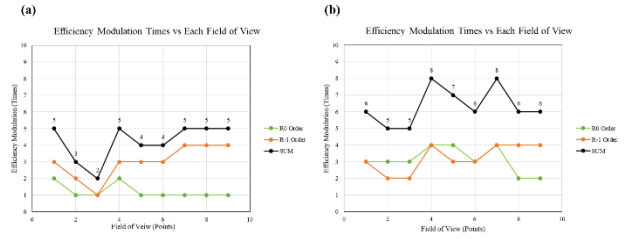

Figure 8. The number of efficiency modulations experienced by the light propagation path through the folding. (a) represents the partitioning based on the propagation path of the R0 grating, while (b) illustrates the partitioning method designed according to the partition angles.

3. SRG Structure by Nanoimprint

In the grating fabrication process, we chose nanoimprint lithography due to its capability of achieving precise dimensional definitions for the distinctly partitioned grating structure design formulas presented in this study. Nanoimprint lithography not only ensures the design accuracy of various grating regions but also effectively meets the demands of large-scale production.

Figure 9 illustrates the waveguide image after imprinting, showing that the angular partitions configured on the folding are successfully and completely transferred to the glass substrate. This process guarantees the integrity and functionality of the grating structure, enabling it to achieve the intended optical performance in practical applications. Additionally, the darker and lighter color variations observed on the folding, resulting from different grating structures, reflect the interference and diffraction effects of light, further demonstrating the success of the fabrication process.

Figure 10 presents scanning electron microscopy (SEM) images of the grating structure, showcasing the results of applying nanoimprint lithography. It can be seen that this technique successfully realized the slanted grating as well as the complete binary grating. These structures not only enhance the design flexibility of optical components but also improve the performance of the waveguide system, laying a solid foundation for future AR applications. With advancements in nanoimprint lithography, we anticipate further expanding the potential of SRG in a broader range of optical applications.

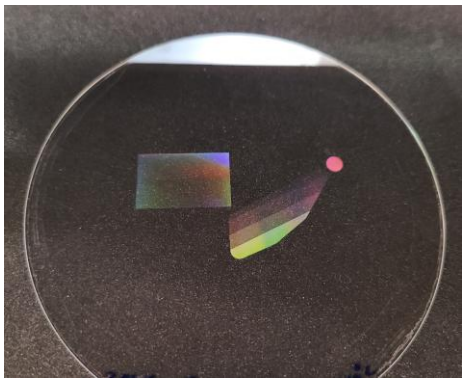

Figure 9. Nanoimprinted SRG waveguide.

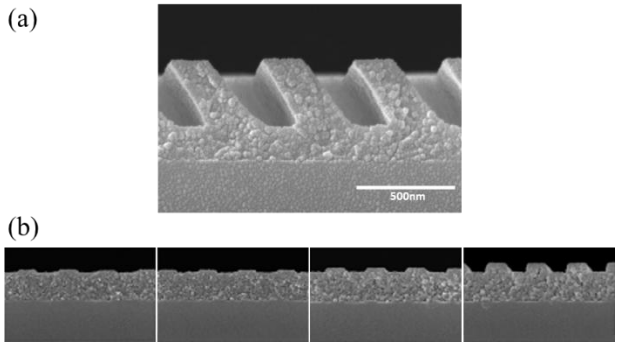

Figure 10. SEM images of the grating structure. (a) represents the slanted grating structure, while (b) show binary structures with different heights, respectively.

4. Optical Performance

Table 1 presents the design specifications for the AR waveguide, which features a field of view (FOV) of 30 degrees. The waveguide achieves a maximum efficiency of 880 nits/lm, with an exit pupil area (Eye-box) of 14 x 8 mm and an eye relief of 20 mm, increasing the user's wearing range.

Figure 11 showcases the optical measurement results of the actual sample, in which we separately injected pure white, red, green, and blue images to evaluate the performance of the waveguide system. During these measurement tests, we calculated the brightness values of different areas using a grid pattern of 9 x 9 points and adopted the ANSI-9 point distribution strategy to compute uniformity using a minimum/maximum (min/max) formula.

The measurement results, as shown in Table 2, reveal that the sample can reach a maximum brightness of 4,583 nits (this value is based on projections from a 5 lm light source projector). In terms of uniformity, the performances for pure white, red, green, and blue images were 49.6%, 42.5%, 41.0%, and 20.1%, respectively. These test results validate the effectiveness of the proposed folding grating partition design in enhancing optical performance and demonstrate its superior brightness uniformity in practical applications.

Specification	Value
Field of view	30°
Eye-Box	12*8 mm
Eye-Relief	20 mm
Brightness efficiency	880 nits/lm

Table 1. Design Specifications for the AR Waveguide.

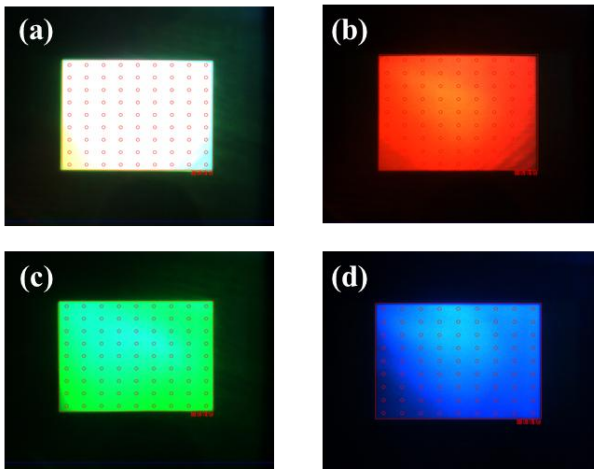

Figure 11. Optical measurement images showing (a) White pattern, (b) Red pattern, (c) Green pattern, and (d) Blue pattern.

#	White	Red	Green	Blue
Max. nits	4,583.4	657.5	3,745.3	211.5
Avg. nits	2,795.2	342.6	2,108.7	112.6
U%	**49.6%**	**42.5%**	**41.0%**	**20.1%**

Table 2. Optical Measurement Results.

5. Conclusion

This study presents an innovative folding partition design method that avoids the efficiency discontinuity effect associated with the out-coupling grating partitioning, while enhancing the modulation space for light at different angles and positions through formula design. It also demonstrates the feasibility of nanoimprint lithography in the fabrication of high-precision grating structures. The optical measurement results from the actual sample show that in tests with pure white images, the sample achieves a maximum brightness of 4,583 nits, with a uniformity measurement result of 49.6%. Additionally, Figure 12 showcases the prototype AR glasses designed for this study. This prototype considers ergonomic factors in its appearance design, aiming to achieve a lightweight and user-friendly wearing experience. In the future, with the rapid advancement of AR technology, our research findings are expected to positively impact the development and application in related fields.

Figure 12. Prototype of the AR Glasses.

6. References

[1] R. T. Azuma, “A survey of augmented reality,” Presence: Teleoperators and Virtual Environments, vol. 6, no. 4, pp. 355-385 (1997).

[2] H. Zhang, Y. Wang, “A Review of Optical Waveguide Technologies for Augmented Reality,” Journal of Display Technology, vol. 15, no. 4, pp. 359-367 (2019).

[3] I. Aharonovich et al., “The role of waveguide technology in the future of augmented reality,” Nature Reviews Materials, vol. 4, no. 5, pp. 1-18 (2019).

[4] B. Wang, L. Zhang, Y. Li, “Design and Optimization of Scalar-Diffraction Gratings for Compact Augmented Reality Systems,” Optics Express, vol. 26, no. 15, pp. 18521-18529 (2018).

[5] Y. Zhang, Y. K. Wang, “Polarization Volume Gratings: A Novel Approach for Optical Devices in Augmented Reality,” Optics Letters, vol. 45, no. 7, pp. 1888-1891 (2020).

[6] H. Hwang, M. H. Lee, J. Kim, “Design and Characterization of Holographic Optical Elements for AR Displays,” Journal of Laboratory Automation, vol. 23, no. 1, pp. 11-22 (2018).

[7] W. Chen, D. Kim, “Nanoprinting Techniques for High-Fidelity Holographic Optical Elements,” Advanced Optical Materials, vol. 8, no. 8, 1902010 (2020).

[8] S. J. Lee, J. Han, “Efficiency and Uniformity in Optical Waveguide Designs: Challenges and Solutions,” Applied Optics, vol. 60, no. 1, pp. 20-30 (2021).

[9] M. Shcherbakov, A. Stepanov, “Uniform Light Distribution in Optical Systems Based on Waveguide Techniques,” Applied Physics Letters, vol. 122, no. 5, 051102 (2023).